



"Ionic Gelation Synthesis, Characterization and Cytotoxic Evaluation of Chitosan Nanoparticles on Different Types of Human Cancer Cell Models"

Marwa A. Ramadan¹, Marwa Sharaky², Amna H. Faid^{3*}

¹Department of laser application in Metrology, Photochemistry and Agriculture, National Institute for Laser Enhanced Science (NILES) Cairo University, Giza, Egypt

² Virology and Immunology Unit, Cancer Biology Department, National Cancer Institute (NCI), Cairo University, Cairo, Egypt

³Department of laser science and interaction, National Institute for Laser Enhanced Science (NILES) Cairo University, Giza, Egypt



Abstract

To study the anticancer effect of chitosan nanoparticles (CSNPs) on a different human cancer cell lines and their possible biomedical application as anticancer, CSNPs were prepared based on the ionic gelation of chitosan with tripolyphosphate anions (TPP). The CSNPs were characterized using UV-VIS spectroscopy, transmission electron microscopy, Fourier transform infrared spectroscopy and zeta analysis. Different human cancer cell lines were used as a model. The cytotoxic effects of the CSNPs on Human breast tumor, human hepatocellular carcinoma, human lung cancer, human colon cancer and human hypopharyngeal were monitored by sulforhodamine B colorimetric assays for cytotoxicity. Treatment of human cancer cell lines with different concentrations of 140 nm diameter of CSNPs produce a concentration dependent decrease in cell viability and IC₅₀ reached about 870 µg mL⁻¹ of CSNPs after 48 h of cell incubation. These investigations implied that CSNPs could be effectively applied to improve the anticancer and nanotherapeutic effect on different types of human cancer cell lines.

Keywords: chitosan nanoparticles (CSNPs), Tripolyphosphate (TPP), Ionic gelation, Cytotoxicity, cancer cell.

1. INTRODUCTION

Cancer is one of the major causes of death all over the world [1]. For most cancer patients Chemotherapy is preferred due to its high efficacy and universality [2]. Nanotechnology shows potential biomedical applications due to its physicochemical properties such as particle size, shape and the charge which enhance the accumulation of nanoparticles in tumor tissues [3]. Chitosan investigated as an efficient drug delivery biopolymer due to Chitosan is biocompatible, biodegradable, nontoxic, and has antimicrobial effect [4, 5]. Chitosan is useful in a variety of applications including biomedicine, pharmaceuticals, metal chelation, and food additives. In addition, the absence of harsh chemicals in the chitosan manufacturing process makes it a promising anticancer drug delivery system [6]. This cationic polysaccharide is soluble in dilute acid and can adhere to the negatively charged biological membranes by electrostatic interaction, thus improving bioavailability and facilitating cell endocytosis [7]. In addition, chitosan has been reported to open the tight junction between epithelial cells, thereby enhancing

the permeability of carried drugs [8]. CSNPs delivered drugs accumulate selectively in tumor, rather than normal, tissues because of an enhanced permeation and retention effect [9]. In addition to its physicochemical properties, surface modifications of CS play a crucial role in the cytotoxic profile and targeting of cancers that are characterized by rapid division and aggressive growth [10]. Jeon and Kim found that chitosan oligomers possess antitumor activity tested both *in vitro* and *in vivo* [11]. *In vitro* CSNPs exerted vigorous cytotoxicity against a colon cancer cell line (Calo320), gastric cancer cell line (BGC823), and liver cancer cell line (BEL7402) [12] and HepG2 [13]. *In vivo*, CSNPs also showed significant dose- and size-dependent antitumor activity against sarcoma-180 and hepatoma H22 in mice. These findings suggest their application as a novel class of drugs against HCC [6].

In this work, CSNPs were synthesized and fully characterized and its nanotherapeutic effect was evaluated after incubation with different human cancer cell lines hoping to prepare biosafe anticancer drugs.

*Corresponding author e-mail: amna_husseini090@yahoo.com.

Receive Date: 27 June 2021, Revise Date: 08 August 2021, Accept Date: 22 August 2021

DOI: 10.21608/EJCHEM.2021.82733.4070

©2022 National Information and Documentation Center (NIDOC)

Material and Methods

Synthesis of Chitosan Nanoparticles (CSNPs)

CSNPs were produced based on ionic gelation method of TPP with chitosan polymer (CS) according to the methodology previously developed [14]. medium molecular weight Chitosan polymer (Sigma-Aldrich, U.S.A.) was dissolved in 0.6% (w/v) with 1% (v/v) acetic acid solution (Sigma-Aldrich, U.S.A.). The pH of chitosan solution was raised to 4.6 – 4.8 with 1N NaOH (99.9%, Sigma-Aldrich, U.S.A.). Chitosan nanoparticles formed spontaneously upon addition of an aqueous TPP (Sigma-Aldrich, U.S.A.) solution 0.3 % (w/v) to the prepared chitosan solutions under magnetic stirring at 800rpm for 30min at room temperature.

Human Cancer Cell Lines

In this study, a panel of the available cell lines was tested for their chemosensitivity. The most sensitive cell line to the treatment regimen was selected. Human breast tumor cell line (T47D, MCF7, SKBR3, MDA-MB-231 and MDA-MB-468), human hepatocellular carcinoma cell line (HepG2), human lung cancer cell line (H460), human colon cancer cell line (HCT116) and human hypopharyngeal cell line (FaDu) were used in this study. It was obtained from the American Type Culture Collection (ATCC, Minnesota, U.S.A.). Cancer cell lines were cultured and maintained in monolayer culture at 37°C under a humidified atmosphere of 5% CO₂ in DMEM media supplemented with 10% fetal bovine serum, 1% antibiotics (penicillin-streptomycin) and 0.5% fungizone. The cells were sub-cultured by trypsinization and maintained in tissue culture laboratory at the National Cancer Institute, Cairo University Egypt.

Cytotoxicity assay

The antitumor activities of (CSNPs) and all tested cell lines cells were evaluated by sulphorhodamine-B (SRB) assay. [15] Briefly, cells were seeded at a density of 3×10^3 cells/well in 96-well microtiter plates. They were left to attach for 24 hours before incubation with CSNPs. Next, cells were treated with different concentrations of (CSNPs) (1000, 2000, 3000 and 4000 ug/ml) for T47D, MCF7, SKBR3, MDA-MB-231, MDA-MB-468, HepG2, HCT116, H460 and FaDu cells. For each concentration, three wells were used and incubation was continued for 48 hours. DMSO was used as control vehicle (1 % v/v). At the end of incubation, cells were fixed with 20 % trichloroacetic acid, stained with 0.4 % SRB dye. The dimethylsulphoxide (DMSO), DMEM medium, fetal Bovine Serum (FBS), trypsin, acetic acid,

sulphorhodamine-B (SRB), trichloroacetic acid (TCA) and trisbase 10mM (PH 10.5) were obtained from Sigma Aldrich Chemical Co., St.Louis, Mo, U.S.A. The optical density (O.D.) of each well was measured spectrophotometrically at 570 nm using ELISA microplate reader (TECAN sunrise™, Germany). The mean survival fraction at each CSNPs concentration was calculated as follows: O.D. of the treated cells/O.D. of the control cells. The IC₅₀ (concentration that produce 50% of cell growth inhibition) value of each CSNPs was calculated using (Graph Pad Prism software, version 5).

Characterization techniques

UV-Visible Spectroscopic Analysis

For absorption measurements, the sample was dissolved in deionized distilled water (DD water) and a 3 mm quartz cuvette was filled with the sample. Spectral absorption was measured using a double beam UV-Vis-NIR spectrophotometer (Cary 5000, Agilent Technologies, Santa Clara. CA. USA).

TEM measurements

The morphologies of the prepared nanostructured materials were investigated using TEM–Nanotechnology & Advanced Material Central Lab (NAMCL), Agriculture Research Center (ARC). Company name: FEI, Netherl and. Model: Tecnai G20, Super twin, double tilt, Applied voltage: 200 kV, Magnification Range: up to 1,000,000 X and Gun type: LaB6 Gun. Drops from a very dilute solution were deposited on an amorphous carbon coated copper grid and left to evaporate at room temperature forming a monolayer then detected by TEM.

Dynamic Light Scattering (DLS) Analysis

The particle size and surface charges of the prepared CSNPs were analyzed through DLS with Zetasizer 300 HAS (Malvern Instruments, Malvern, UK) based on photon correlation spectroscopy. Analysis time was 60 s and the average zeta potential was determined. The zeta potential of nanoparticulate dispersion was determined as such without dilution.

FTIR analysis

FTIR measurements were carried out using FT-IR spectrometer (4100 Jasco-Japan) in the range (500 – 4500 cm⁻¹). CS, TPP and CSNPs were freeze dried using lyophilizer. IR spectra of powdered samples were diluted with a potassium bromide (KBr) pellet and then measured.

Statistical analysis

Statistical analysis was carried out using (Graph Pad Prism software, version 5) Software.

Results and Discussion

The preparation of CSNPs based on an ionic gelation interaction between positively charged CS and negatively charged TPP. Formation of nanoparticles occurs spontaneously through the formation of intra- and intermolecular cross-linkages under a constant stirring at ambient temperature.

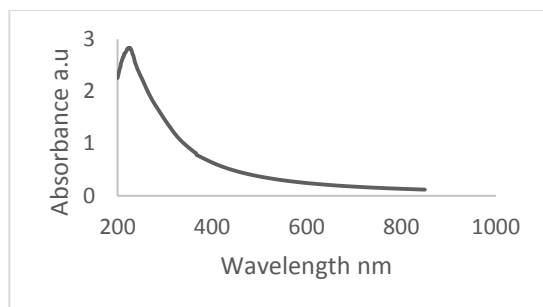


Figure 1: UV-Vis absorption band for CSNPs

As shown in figure 1. UV-Vis absorption band for CSNPs, the band 200-300 nm indicates the presence of a CO group in the CSNPs[16].

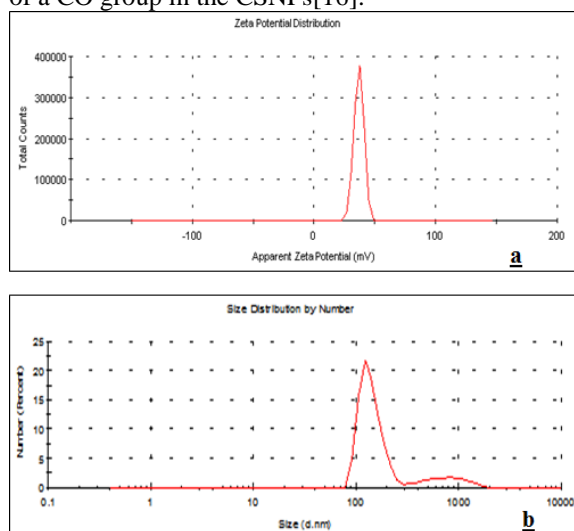


Figure 2: Zeta potential (a) and zetasizer (b) of chitosan nanoparticles.

Zeta potential of CSNPs can greatly influence their stability in suspension by means of electrostatic repulsion between the particles[17]. The respective average diameter and zeta potential measured by Zetasizer for CSNPs was ranging from 70-140 nm and 36.9 ± 4.11 mV.

TEM images of CSNPs are shown in Figure 3; CSNPs are nearly spherical shape and its size range from 70-140nm which confirms the diameters measured by Zetasizer.

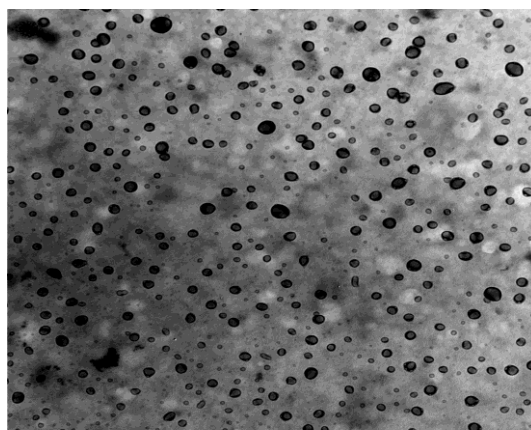


Figure 3: TEM image of CSNPs

FTIR analysis of CS, TPP and CSNPs were performed to characterize the chemical structure of the prepared nanoparticles. As shown in Figure 4 and table 1, the characteristic peaks of CS are peaks at 3436 cm^{-1} attributed to hydrogen-bonded O-H stretching vibration, the peaks of N-H stretching from primary amine and type II amide are overlapped in the same region, the peak at 1652 cm^{-1} is attributed to the CONH_2 group, while The peak at 1370 cm^{-1} is attributed to the bending vibration of C-H deformation and the peak at 1081 cm^{-1} corresponding to $\nu(\text{C-O-C})$ [18]. In TPP spectrum following characteristic peaks can be observed: 1214 cm^{-1} is assigned to P=O stretching, peak at 1148 cm^{-1} is corresponding to symmetric and antisymmetric stretching vibrations in PO_2 group, more over peak at 1093 cm^{-1} is attributed symmetric and antisymmetric stretching vibrations in PO_3 group and peak at 912 cm^{-1} is revealed to antisymmetric stretching of the P-O-P bridge). The spectrum of CSNPs is different from that of chitosan polymer. In CSNPs, the peak at 3436 cm^{-1} in chitosan polymer shifted to 3423 cm^{-1} and becomes wider with increasing in relative intensity this indicated that hydrogen bonding is enhanced, peak at 1652 cm^{-1} in chitosan polymer shifts to 1642 cm^{-1} and its intensity decreased and a new sharp peak at 1549 cm^{-1} corresponding to N-H (Bend) appears. CSNPs also shows a P=O peak at 1154 cm^{-1} . These results can be attributed to the linkage between phosphoric group of TPP and ammonium group of chitosan in nanoparticles which serves to enhance both inter- and intramolecular interaction in CSNPs[19]. The terminal phosphate group of TPP binds with amine NH_2 group of chitosan by ionic bond. The ionic interaction with the phosphate group of TPP indicated the conversion of chitosan polymer into CSNPs that forms a cross link with TPP. The strong and sharp peak of phosphate at 1084 cm^{-1} in CSNPs confirmed the involvement of TPP during the nanoparticles creation[20].

Table 1. The main characteristic peaks of the chitosan polymer CS, TPP and CSNPs.

Material	Wavenumber (cm ⁻¹)	Assignment
CS	3436	N-H stretching vibration overlapped with -OH stretching vibration.
	1652	C=O of amide group -CONH ₂ .
	1370.	Bending vibration of C-H group
	1081	C-O stretching vibration
TPP	1214	Stretching vibration of P=O.
	1148	symmetric and antisymmetric stretching vibrations in PO ₂ group)
	1093	symmetric and antisymmetric stretching vibrations in PO ₃ group
	912	anti-symmetric stretching of the P-O-P bridge
CSNPs	3423	Broad N-H stretching vibration overlapped with -OH stretching vibration.
	1549	to N-H (Bend)
	1642	N-H (Bend)
	1154	P=O

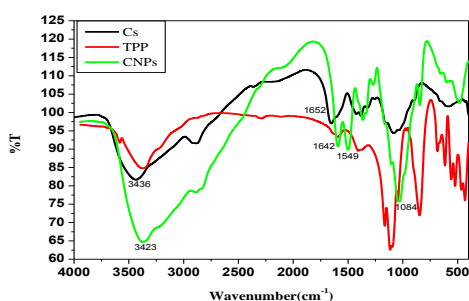


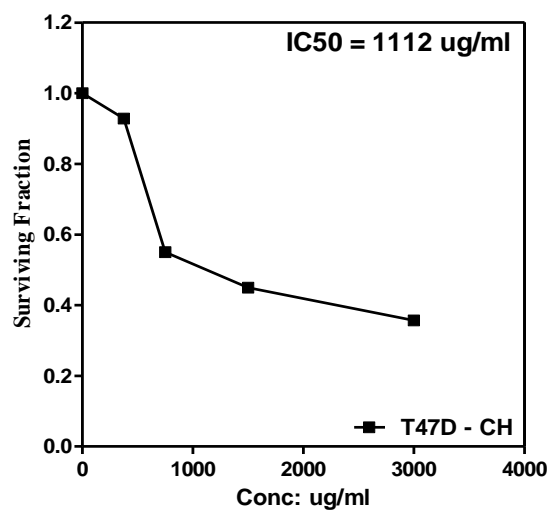
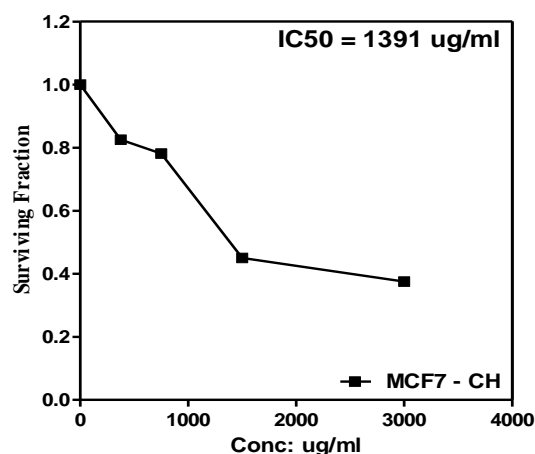
Figure 4: FTIR spectra of CS, TPP and CSNPs

Effect of different concentration of CSNPs on cellular proliferation of different cell lines.

To examine the antitumor activity on (T47D, MCF7, SKBR3, MDA-MB-231, MDA-MB-468, HepG2, HCT116, H460 and FaDu cells) exponentially dividing cells were treated with different concentrations of CSNPs (1000, 2000, 3000 and 4000 ug/ml), the cell viability was measured as shown in Fig. 5. There was a concentration dependent decrease in cellular proliferation compared to its respective control. It was observed that CSNPs produce a significant decrease in all cells with IC₅₀ as shown in figure 6, which is improve the effectiveness of CSNPs by reducing the cytotoxicity by nearly half.

Our results were in accordance with a previous research results of Y. Xu and coworkers[6] which conclude that chitosan nanoparticles (CNPs) could inhibit the growth of human hepatocellular carcinoma through a mechanism of CNP-mediated inhibition of tumor angiogenesis that was associated to impaired levels of vascular endothelial growth factor receptor 2 (VEGFR2). Nam and coworkers have found that the treatment of MDA-MB-231 human breast carcinoma cells with increasing concentration of chitosan inhibited the migration of these cells through

membrane because this combination of chitosan and carcinoma cell lines lowered the activity and amount of MMP9 protein and this anti metastatic behavior increased with increase in Chitosan concentration. [21]



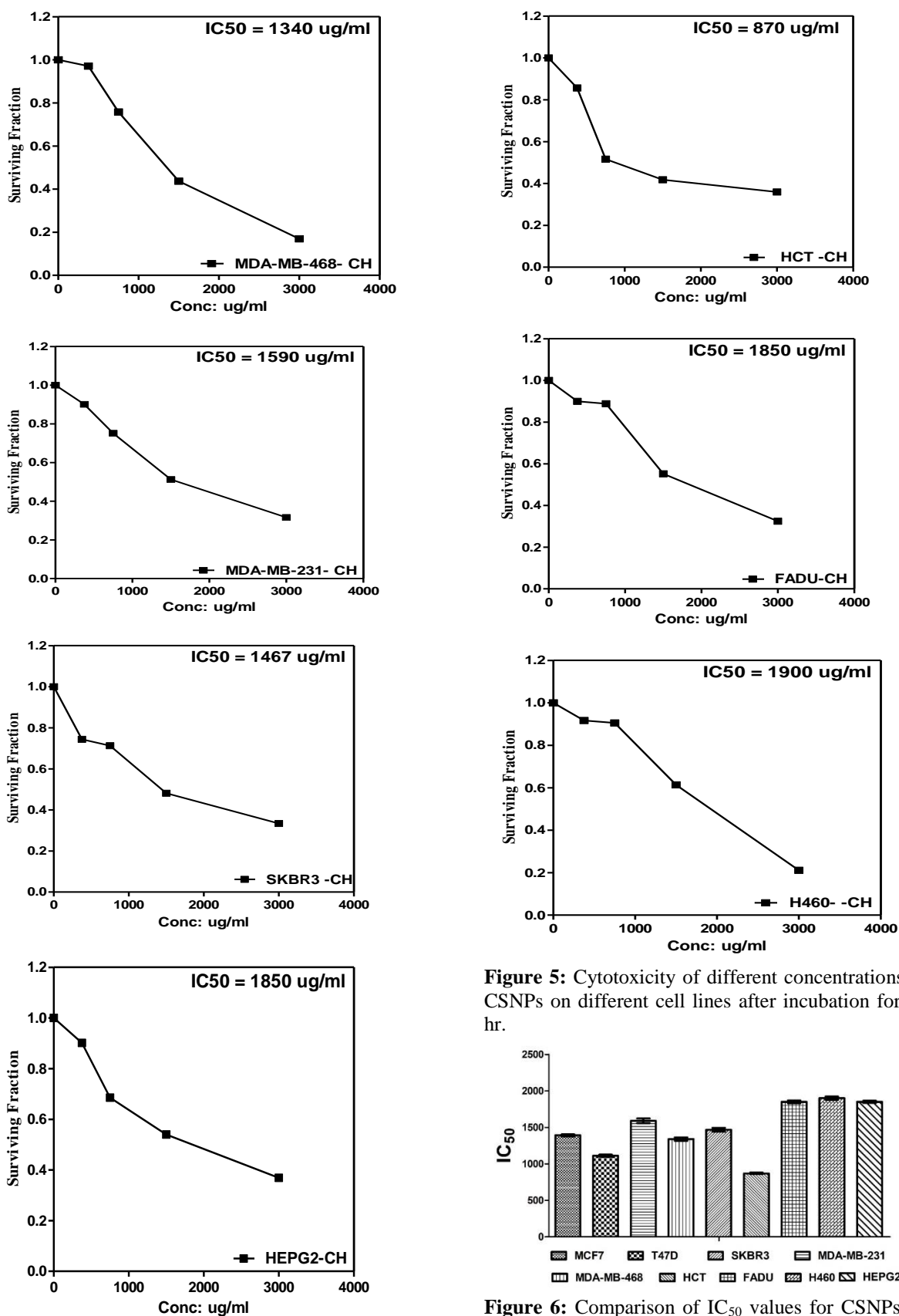


Figure 5: Cytotoxicity of different concentrations of CSNPs on different cell lines after incubation for 48 hr.

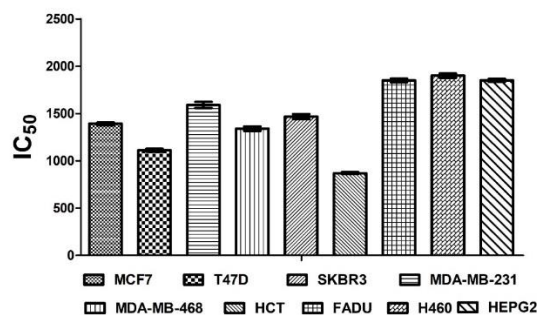


Figure 6: Comparison of IC₅₀ values for CSNPs on different cell lines after at 48hr

Nanoparticles can inhibit the proliferation of cancer cells and the apoptosis of cancer cells is associated with reactive oxygen species (ROS) mediated pathways. The ROS generation capability of nanoparticles is related to the cytotoxic response in various cell types. It was found that the internalization of CSNPs specifically occurred at the mitochondria and increased ROS generation, thus resulting in activation of ROS induced mitochondrial disorders [22, 23]. In future research work further analysis at the molecular level are still required to evaluate impact of CNPs to confirm our results and facilitate biomedical applications *in vivo*.

Conclusion

The current study used an ionic gelation approach to synthesis chitosan nanoparticles in a quick, highly stable, and low-cost manner. The impact of CSNPs on several human cancer cell lines was investigated. Our results revealed that CSNPs reduce cell viability in a concentration-dependent manner, reaching IC₅₀ in all cell lines tested. Future research is being carried out to look at the favorable effects Chitosan Nanoparticles in drug delivery and *in vivo* studies.

References

1. Bray, F., et al., *Global cancer statistics 2018: GLOBOCAN estimates of incidence and mortality worldwide for 36 cancers in 185 countries*. CA: A Cancer Journal for Clinicians, 2018. **68**(6): p. 394-424.
2. Al-Batran, S.-E., et al., *Perioperative chemotherapy with fluorouracil plus leucovorin, oxaliplatin, and docetaxel versus fluorouracil or capecitabine plus cisplatin and epirubicin for locally advanced, resectable gastric or gastro-oesophageal junction adenocarcinoma (FLOT4): a randomised, phase 2/3 trial*. The Lancet, 2019. **393**(10184): p. 1948-1957.
3. Bastiancich, C., et al., *Anticancer drug-loaded hydrogels as drug delivery systems for the local treatment of glioblastoma*. Journal of Controlled Release, 2016. **243**: p. 29-42.
4. Nezakati, T., et al., *Conductive Polymers: Opportunities and Challenges in Biomedical Applications*. Chemical Reviews, 2018. **118**(14): p. 6766-6843.
5. Guo, H., et al., *Preparation and Characterization of Chitosan Nanoparticles for Chemotherapy of Melanoma Through Enhancing Tumor Penetration*. Frontiers in Pharmacology, 2020. **11**(317).
6. Xu, Y., Z. Wen, and Z. Xu, *Chitosan Nanoparticles Inhibit the Growth of Human Hepatocellular Carcinoma Xenografts through an Antiangiogenic Mechanism*. Anticancer Research, 2009. **29**(12): p. 5103.
7. Kwak, S., et al., *The Immediate and Sustained Positive Effects of Meditation on Resilience Are Mediated by Changes in the Resting Brain*. Frontiers in Human Neuroscience, 2019. **13**(101).
8. Sheng, J.-X., et al., *Global atmospheric sulfur budget under volcanically quiescent conditions: Aerosol-chemistry-climate model predictions and validation*. Journal of Geophysical Research: Atmospheres, 2015. **120**(1): p. 256-276.
9. Brannon-Peppas, L. and J.O. Blanchette, *Nanoparticle and targeted systems for cancer therapy*. Advanced Drug Delivery Reviews, 2004. **56**(11): p. 1649-1659.
10. Cheng, L., et al., *Synthesis of folate-chitosan nanoparticles loaded with ligustrazine to target folate receptor positive cancer cells*. Molecular medicine reports, 2017. **16**(2): p. 1101-1108.
11. Kim, S.-K. and N. Rajapakse, *Enzymatic production and biological activities of chitosan oligosaccharides (COS): A review*. Carbohydrate Polymers, 2005. **62**: p. 357-368.
12. Qi, L., et al., *Cytotoxic activities of chitosan nanoparticles and copper-loaded nanoparticles*. Bioorganic & Medicinal Chemistry Letters, 2005. **15**(5): p. 1397-1399.
13. Loutfy, S.A., et al., *Synthesis, characterization and cytotoxic evaluation of chitosan nanoparticles: in vitro liver cancer model*. Advances in Natural Sciences: Nanoscience and Nanotechnology, 2016. **7**: p. 1-9.
14. Furtado, G.T., et al., *Chitosan/NaF Particles Prepared Via Ionotropic Gelation: Evaluation of Particles Size and Morphology*. Materials Research-ibero-american Journal of Materials, 2018. **21**.
15. Skehan, P., et al., *New Colorimetric Cytotoxicity Assay for Anticancer-Drug Screening*. JNCI: Journal of the National Cancer Institute, 1990. **82**(13): p. 1107-1112.
16. Vaezifar, S., et al., *Effects of Some Parameters on Particle Size Distribution of Chitosan Nanoparticles Prepared by Ionic Gelation Method*. Journal of Cluster Science, 2013. **24**(3): p. 891-903.

17. Mohammadpour Dounighi, N., et al., *Preparation and in vitro characterization of chitosan nanoparticles containing Mesobuthus eupeus scorpion venom as an antigen delivery system*. Journal of Venomous Animals and Toxins including Tropical Diseases, 2012. **18**: p. 44-52.
18. Ibrahim, H., et al., *Preparation of Chitosan Antioxidant Nanoparticles as Drug Delivery System for Enhancing of Anti-Cancer Drug*. Key Engineering Materials, 2018. **759**: p. 92-97.
19. Lazaridou, M., et al., *Formulation and In-Vitro Characterization of Chitosan-Nanoparticles Loaded with the Iron Chelator Deferoxamine Mesylate (DFO)*. Pharmaceutics, 2020. **12**(3).
20. Kahdestani, S.A., M.H. Shahriari, and M. Abdouss, *Synthesis and characterization of chitosan nanoparticles containing teicoplanin using sol-gel*. Polymer Bulletin, 2021. **78**(2): p. 1133-1148.
21. Kyung-Soo, N., *Suppression of Metastasis of Human Breast Cancer Cells by Chitosan Oligosaccharides*. Journal of Microbiology and Biotechnology, 2009. **19**(6): p. 629-633.
22. Jiang, Y., et al., *Chitosan nanoparticles induced the antitumor effect in hepatocellular carcinoma cells by regulating ROS-mediated mitochondrial damage and endoplasmic reticulum stress*. Artificial Cells, Nanomedicine, and Biotechnology, 2019. **47**(1): p. 747-756.
23. Adhikari, H.S. and P.N. Yadav, *Anticancer Activity of Chitosan, Chitosan Derivatives, and Their Mechanism of Action*. International Journal of Biomaterials, 2018. **2018**: p. 2952085.